The International Journal of Advanced Manufacturing Technology (2024) 133:5117–5126
https://doi.org/10.1007/s00170-024-14041-5

ORIGINAL ARTICLE

Effect of moisture content on the mechanical performance of 3D printed continuous reinforced two-matrix composite

Marina Andreozzi[1] · Serena Gentili[1] · Pietro Forcellese[2] · Tiziano Bellezze[2,3] · Valeria Corinaldesi[2,3] · Francesca Luzi[2,3] · Alessio Vita[1]

Received: 22 March 2024 / Accepted: 17 June 2024 / Published online: 29 June 2024

Abstract

Additive manufacturing, particularly Fused Filament Fabrication, has gained significant attraction in recent years. In order to increase the mechanical performances of several components, continuous reinforcements, such as carbon fibers, can be coextruded with a polymeric matrix.

The present study relies on a specific 3D printing process, called towpreg coextrusion, which exploits continuous carbon fibers covered with an epoxy resin and polyamide (PA) as the thermoplastic matrix, thus obtaining a 3D printed two-matrix composite. Since polyamide is a highly hygroscopic material, the impact of moisture content on the mechanical properties of 3D-printed continuous composites was investigated. Tensile and flexural specimens were manufactured and tested under both undried and dried conditions. Drying treatment was carried out at a temperature of 70 °C for 2 h in oven, with weight measurements before and after for quantifying weight loss and then the moisture removal. Additionally, through thermogravimetric analysis, the thermal stability of the material was assessed. It was observed that the drying process allows for a reduction of up to 0.56% by weight of moisture in the specimens. Thus, the drying process led to an improvement in the mechanical properties of the material. Specifically, the tests reveal a 15% increase in tensile strength and an 11.5% increase in flexural strength following the drying process, reaching values of 392.78 MPa and 151.06 MPa, respectively. Similarly, an increase in the tensile and flexural moduli was noted in the treated specimens. Finally, fractured samples underwent optical and scanning electron microscopy analysis, through which different fracture mechanisms of the material and the presence of macrovoids and microvoids attributable to the 3D printing process were observed. Knowledge of deposition defects represents an important starting point for the improvement of the process and the mechanical properties obtained to date. This research provides valuable insights into optimizing 3D-printed continuous composites, emphasizing the importance of moisture control for superior mechanical performance in industrial applications.

Keywords Additive manufacturing · Coextrusion process · Two-matrix composite materials · Moisture effect · CFRP · TGA

1 Introduction

Additive manufacturing has shown remarkable progress in recent years; in particular, Fused Filament Fabrication (FFF) has emerged as the leading technique in 3D printing technologies [1, 2]. FFF, known for its versatility and cost-effectiveness, has received widespread attention for its applicability in various fields. One of the main limitations of this technology is the achievable mechanical performance. Indeed, even if toughened thermoplastics or techno-polymers are used (such as PA or PEEK), it is difficult to reach tensile strength higher than 100 MPa [3]. A method to reinforce 3D printing filament is to produce a composite by adding short

Highlights
- Tensile and flexural specimens were printed using a 3D printing process with continuous carbon-epoxy filament (CCF) and a nylon-based material as the thermoplastic matrix.
- The impact of moisture content on the mechanical properties of 3D-printed continuous composites was investigated.
- Drying treatment was carried out.
- Thermogravimetric and scanning electron microscopy analyses have been performed.
- The drying process improves mechanical properties.

Marina Andreozzi and Serena Gentili made equal contribution.

Extended author information available on the last page of the article

carbon fibers [4]. In this way, it is possible to increase the performances of 3D-printed components, also reaching tensile strength higher than 150 MPa. However, these values are not sufficient for different industrial applications where high performances are mandatory. Another possibility to obtain much higher performances is to manufacture a 3D-printed composite with continuous fibers [5, 6]. The study conducted by Dul et al. [7] found that specimens printed in PA with continuous carbon fiber achieved 34% higher tensile performance in strength and 147% higher stiffness than pure PA. In bending, they also found an increase in strength and stiffness of 29% and 140%, respectively.

The use of continuous fibers in these technologies has received significant attention, with the development of numerous successful prototypes and commercial printers [8–10].

Given the growing interest in the 3D printing of continuous fiber composites, a significant increase in the employed technologies has been reported in recent years [11]. Currently, the range of printable materials, the size of produced parts, achievable production volumes, and application fields have expanded. As of today, a formal classification of long-fiber composite printing techniques does not exist. However, it is possible to categorize the processes based on how the fiber and matrix are directed to the printing nozzle and how they are deposited [12, 13].

In the in-situ impregnation technologies, dry fibers are pushed through the nozzle, in which they are impregnated with the matrix, thus realizing the coextrusion process. Two other existing technologies are in-line impregnation and in-situ consolidation. In the former, the fiber is impregnated while being pushed through the nozzle. In the latter, however, a thermoplastic filament (towpreg) is consolidated in situ by a pressure roller during deposition, while an external heat source facilitates polymerization. When the preimpregnated filament is directly heated and extruded trough the nozzle, the relative manufacturing technology is named towpreg extrusion[14]. Another technique is the coextrusion of towpreg. In this case, instead of dry fiber, a thin towpreg/preimpregnated filament is used, heated, and coextruded together with the matrix. If the towpreg matrix is the same as the coextrusion matrix, a monomatrix composite is obtained and, if the matrix filament material is a thermoplastic, the approach is referred to as continuous fiber-reinforced thermoplastic composites [10, 15]. On the contrary, a bimatrix composite is referred to when the resin used for tow fabrication differs from the coextrusion resin [16–18]. An example is the coextrusion of thermoplastic resin and preimpregnated thermosetting resin carried out by the Composer 3D printer developed by Anisoprint. This system exploits a 1.5-K continuous carbon fiber filament impregnated with an epoxy resin and PA as the main thermoplastic matrix. The carbon fiber filament is reinforced with the thermoset resin through a patented binderization process in order to increase its processability in the 3D printer. The binderization process aims to provide more stiffness to the filament, thus avoiding the fluffing of the fibers during the movements. However, once the fiber bundle crosses the heated nozzle, the thermoset resin is heated at a temperature higher than its glass transition temperature, thus allowing an easy deposition of the fibers also in curved geometries. Furthermore, in the heated nozzle , the impregnation of the fiber bundle with the thermoplastic polyamide occurs. This phase is crucial to obtain high-quality components without defects such as voids. In fact, in the case of 3D-printed composite structures, it is very important to explore the surface topology, cross-sectional view, and nature of the fracture to understand whether structural defects such as gaps and poor interlaminar adhesion are present [11]. Indeed, the presence of voids leads to a decrease in mechanical performances as they act as nucleation points for cracks. A parametric study of a type of continuous two-matrix carbon fiber composite constituted by PET-G and prepreg carbon fiber bundles, using coextrusion of towpreg technology [16], showed an increase in maximum flexural strength and modulus of 74% and 93% over those of pure PETG parts, and the minimum porosity content of 3.19% is achieved. The presence of voids within the molded CF/PA6 continuous composite was found to have a substantial negative impact on mechanical performance, as transverse tensile strength and flexural strength increased by 78% and 93%, respectively, with the void content decreasing from 12 to 6% [19]. In addition, voids typically increase moisture absorption, another aspect that can lead to a reduction in performances. Moreover, PA is known for its high hygroscopicity, which predisposes it to absorb moisture during the 3D printing process [20, 21]. No scientific research can be found concerning the effect of moisture absorbed by the polyamide material on the mechanical performances of 3D-printed continuous composites.

In this framework, the present study aims to address a critical knowledge gap by investigating the effect of moisture content on the mechanical performances of 3D-printed continuous fiber composites fabricated using the towpreg coextrusion process. In this context, no prior research has explored this relationship. Thus, this study will provide novel insights in relation to how moisture absorption in the polyamide matrix influences the mechanical properties of 3D-printed structures.

The aim of this research was fulfilled by conducting tensile and flexural characterization on specimens manufactured with the towpreg coextrusion. Specimens will be tested in both undried and dried conditions (moisture removed through heating at 70 °C for 2 h). The thermogravimetric analysis will be conducted to assess the thermal stability of the materials, and the amount of moisture removed will be quantified by weighing samples before and after drying.

Undried samples will be tested immediately after 3D printing. Finally, fractured samples will be analyzed using optical and scanning electron microscopy (SEM) to investigate the presence and influence of voids on mechanical performance.

2 Materials and methods

2.1 3D printer and material

The machine used for the 3D printing of continuous fiber-reinforced composites was the Composer A3 printer developed by Anisoprint Inc. This system exploits the additive manufacturing process illustrated schematically in Fig. 1. This process allows to 3D print a composite material consisting of continuous carbon fibers and a thermoplastic matrix. Thus, inside the heated chamber, the thermoplastic material is melted and extruded simultaneously with the continuous filament through the same extrusion nozzle. For this reason, the process is called composite fiber coextrusion (CFC). The utilization of dedicated cutting equipment enables the segmentation of continuous fibers, thus facilitating the fabrication of geometrically complex and dimensionally precise structures.

As far as the continuous carbon-epoxy filament (CCF) is concerned, it was supplied by the machine manufacturer and consists in a tow of 1.5-K carbon fibers with an average diameter of 7 µm. In order to increase the stiffness and the processability of the CCF, the tow is covered, through a binderization process, with an epoxy-based thermoset resin. This CCF filament has remarkable mechanical properties, including an elastic modulus of 150 GPa, a tensile strength of 2200 MPa, and a carbon fiber volume fraction of 60%, as reported in the technical datasheet provided by the manufacturer.

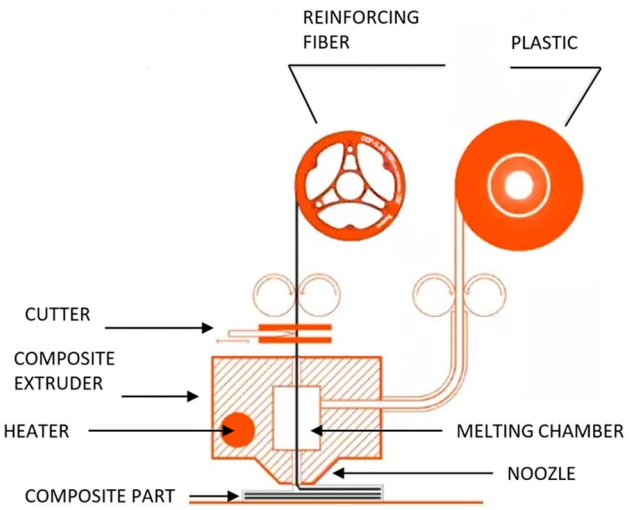

Fig. 1 Scheme of CFC process

Concerning the thermoplastic matrix, the Anisoprint CFC process exploits a specially developed nylon-based material from Polymaker. This resin is characterized by a tensile and flexural strength of 57 MPa and 69 MPa, respectively; an elastic modulus in tension and flexure of 1440 MPa and 1580 MPa, respectively; and an elongation at break of 15.86%. In addition, this resin exhibits a low-viscosity profile, enhancing the interlayer adhesion of the fibers. Moreover, its quick cooling and solidification properties contribute significantly to the precision of fiber placement, ensuring enhanced quality in the final component. This resin is characterized by a low absorption of moisture.

The 3D printing process started with the design of the CAD geometries using dedicated software. Then, the generated mesh files were imported into the proprietary slicing software (Aura) that converted the 3D models into instructions for the 3D printer, generating a GCODE file. Aura software allows the configuration of various printing parameters, including infill, flow multiplier, reinforced infill pattern, guide direction, printing speed, and printing temperature (Table 1).

The printing parameters, as recommended by the Anisoprint experts, were chosen to optimize the mechanical properties of the 3D-printed specimens. Additionally, the implementation of a solid-reinforced infill pattern ensures a 100% infill with continuous carbon fiber, significantly enhancing the characteristics of the components.

2.2 Thermogravimetric analysis

The thermal stability of the preimpregnated fiber bundle and composites (5–10 mg) was investigated through thermogravimetric analysis (TGA), using TA Instruments, TGA 55 equipment, at a heating rate of 10 °C min^{-1} from 40 to 900 °C in a nitrogen gas atmosphere (100 mL min^{-1}). The composite specimens, before being submitted to this analysis, were stored at two different conditions, to examine the effect of humidity absorption: some of them were stored at room temperature (RT) and maintained at room humidity (undried); the remaining specimens were dried in an oven at 70 °C for about 2 h (dried). The drying treatment was

Table 1 Printing parameters

Average printing speed	6 mm/s
Reinforced infill pattern	Solid
Macrolayer height	0.32 mm
Extrusion width	0.65 mm
Extruder temperature	250 °C
Build plate temperature	60 °C

applied also for the PA. For TGA analyses, samples of these different composite specimens and those of PA were used.

2.3 Drying procedure

To analyze the effect of moisture on the properties of 3D-printed composites, mechanical tests were conducted on both dried and undried specimens. The drying process, aimed at moisture removal, involved a specific exsiccation method. It consists of placing the 3D-printed samples in a ventilated oven at a temperature of 70 °C for 2 h. The effectiveness of this drying procedure was quantitatively assessed by measuring the weight of the samples before and after drying using an analytical balance with a resolution of 0.005 g.

2.4 Tensile test

To assess the mechanical performances of the 3D-printed composites, tensile tests were carried out. The test specimens were fabricated in accordance with ASTM D3039 standards: 2 mm in thickness, 15 mm in width, and 250 mm in length. To prevent potential defects due to the curving of continuous fibers at the specimen ends, an elliptical-shaped geometry was adopted (as depicted in Fig. 2) and the tensile specimens were cut from the rectilinear part of the 3D-printed sample. As can be seen from the figure, the fibers were oriented in the direction of the tensile load, thus allowing for the highest achievable tensile properties.

To guarantee repeatability, different tensile specimens were printed and tested. More in detail, 4 samples were printed and tested immediately after printing while the other 4 samples were subjected to the drying process reported in Sect. 2.4 before testing. This allows us to investigate the effect of moisture on the tensile properties of the 3D-printed composites. The tensile tests were conducted using a Zwick/Roell Z050 machine with a constant test speed of 2 mm/min. During the testing process, a 50-kN load cell was utilized to measure the applied load, while an optical extensometer was employed to record the nominal strain along the loading direction, by which the maximum value of tensile strength was calculated.

2.5 Flexural test

The flexural behavior of the 3D-printed composite was characterized through a three-point bending test. The test was conducted following the ASTM D7264 standard, and the specimen dimensions were 128 mm in length, 4 mm in thickness, and 15 mm in depth. The span-to-thickness ratio was 32:1.

In this case, specimens were fabricated using a rectangular geometry, sized in accordance with the standard, with an initial fiber protrusion in order to reduce the risk of fiber under-extrusion that can lead to missing fibers in the specimen during the initial printing phase.

The extruded part visible at the sample corner indicates the onset of the 3D printing process, a technique employed to ensure uniform fiber distribution throughout the specimen. After the printing process and prior to mechanical testing, these protrusions are dedicated tools.

A universal testing machine equipped with a 25-kN load cell was used to perform the tests. According to the standard, a loading nose and supports of 5-mm radii were employed, and the crosshead speed was set to 2 mm/min. During the test, the load and displacement (with contact microestensimeter) were recorded. The stress and the strain for any point on the load-deflection curve were calculated following the ASTM D7264, Procedure A. The flexural modulus was calculated as the slope of the stress-strain curve taken in the strain range between 0.001 and 0.003.

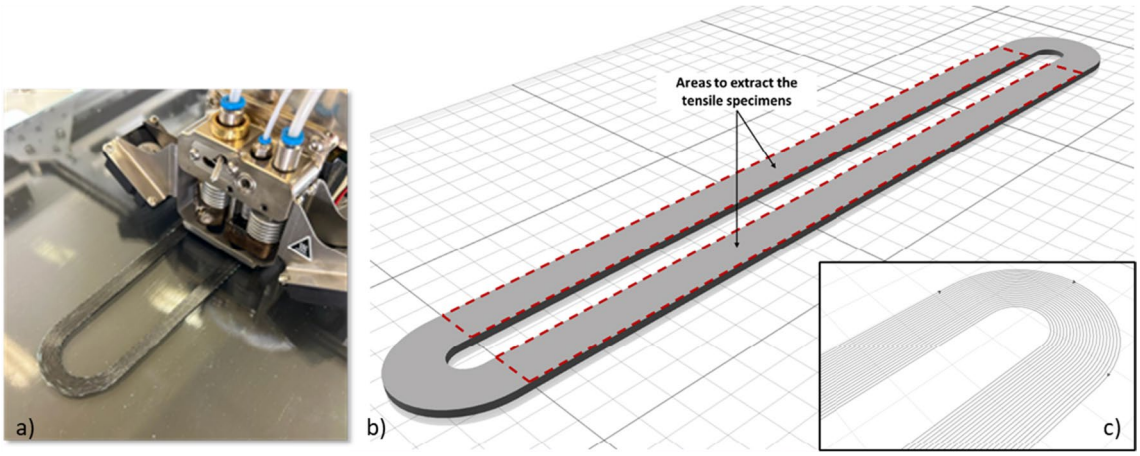

Fig. 2 **a**) Tensile specimen process. **b**) Areas of the elliptical shape to extract the tensile specimens. **c**) Scheme of the carbon fiber composite deposition

Also, in this case, a total of 8 specimens were 3D printed. Four samples were tested immediately after printing, while the other 4 were subjected to the moisture removal procedure reported in Sect. 2.4.

2.6 Optical and scanning electron microscopies

The morphological analysis of the fracture surfaces from specimens subjected to flexural and tensile tests was conducted using the Leica DMi8 optical microscope (Leica Microsystems GmbH, Wetzlar, Germany). Additionally, for more detailed inspection, the SEM EVO 10 was employed to achieve high-resolution imaging of the fractured surfaces of the tested specimens. Prior to the SEM observations, the specimens underwent a gold metallization process to enhance conductivity and facilitate the acquisition of high-quality electron microscope images, then observed using an accelerating voltage of 20 kV.

2.7 Statistical analysis

Mechanical measurements were reported as mean ± standard deviation (mean ± SD). One-way ANOVA test was used for statistical analysis using the Statgraphics Plus 5.1. Program (Manugistics Corp., Rockville, MD). To differentiate samples, Fisher's least significant difference (LSD) was used at the 95% confidence level. Differences were considered statistically significant for $p < 0.05$.

3 Results and discussion

3.1 Thermogravimetric analysis

Figure 3 shows the residual mass and the corresponding derivative of a sample of the impregnated fiber bundle (Fig. 3(a)); these curves are reported also in Fig. 3(b) and (c) together with those of PA and undried and dried composites. The initial weight loss of preimpregnated fiber bundle starts from 230 °C (symbolized as T_0 in Fig. 3(a)), which is related to the initial thermal decomposition behavior of the epoxy resin. It follows with a 5 wt% weight loss (T_{onset} fiber bundle) at 365 °C according to the literature [16]. The thermal decomposition is due to the cleavage of aromatic groups in the epoxy matrix, and the main degradation peak is centered at 415 °C. At 600 °C, a reduction in material weight of about 30% has been calculated (Fig. 3(a)). Therefore, the weight fraction of carbon fiber is close to 70% (Fig. 3(a)).

TGA measurements of the fiber bundle, thermoplastic polymer, and dried and undried composites are displayed in Fig. 3(b), (c). The TG (Fig. 3(b)) and DTG (Fig. 3(c)) curves of both composites show similar thermo-degradative behavior. The presence of multi-degradation steps in composite specimens indicates the presence of different components characterized by different temperatures of decomposition. The first residual mass step of the undried composite sample (see inset in Fig. 3(b)) is due to the presence of moisture that can be removed at a temperature below 130 °C. The corresponding weight loss is estimated at around 0.50% (residual mass loss is close to 99.5%). This result is in agreement with those of Tables 2 and 3, thus confirming the presence of a small amount of water in the undried composites, which influences their mechanical properties, as reported above.

The main peak of DTG curves corresponds to a mass loss at 454 °C (Fig. 3(c)), as a result of the thermal degradation behavior of PA, clearly present also in the composites [22]. In addition, in the composite curves, also a shoulder can be observed at 384 °C. This value is a little bit less than that of the DTG peak at 415 °C of the stand-alone epoxy resin in the fiber bundle, suggesting that the degradation process of this resin is made more complicated by the contact with the PA matrix.

Finally, at 900 °C, the residual mass of PA was estimated at 1.7%, while for composites 46.6% and 45.8% for undried and dried (Fig. 3(c)), respectively. This last variation can be attributed to the different polymer content in the samples analyzed by TGA, as a consequence of slightly different amounts of polymers deposited on carbon fibers during the 3D printing process, according to the SEM analysis (Fig. 7).

3.2 Tensile tests

Figure 4 shows the typical nominal stress vs. nominal strain curves obtained by performing tensile tests on undried and dried specimens.

In Table 2, the average value of maximum tensile strength (σ_{tmax_avg}), tensile strain at the peak stress point (ε_{tmax_avg}), Young's modulus (E_{t_avg}), and the respective standard deviations are reported. Furthermore, the average weight loss related to moisture removal is also reported.

From the results, it can be observed that the drying process led to an average weight reduction of 0.5% and an enhancement in mechanical properties. Indeed, the tensile stress of dried materials exhibited a 15% increase while no significant differences ($p < 0.05$) of tensile Young's modulus and tensile deformation at break were registered.

The increase of both tensile strength and elastic modulus after the drying process is confirmed by literature. Polyamide is well known for its hygroscopic nature and the moisture absorption results in a hydrolytic degradation of the polymer, particularly at the interface with the reinforcing fibers [21, 23, 24]. The drying process minimizes this degradation, preserving the structural integrity of the polymer and the fiber-matrix interface. This preservation is fundamental to guarantee an effective stress transfer mechanism from the

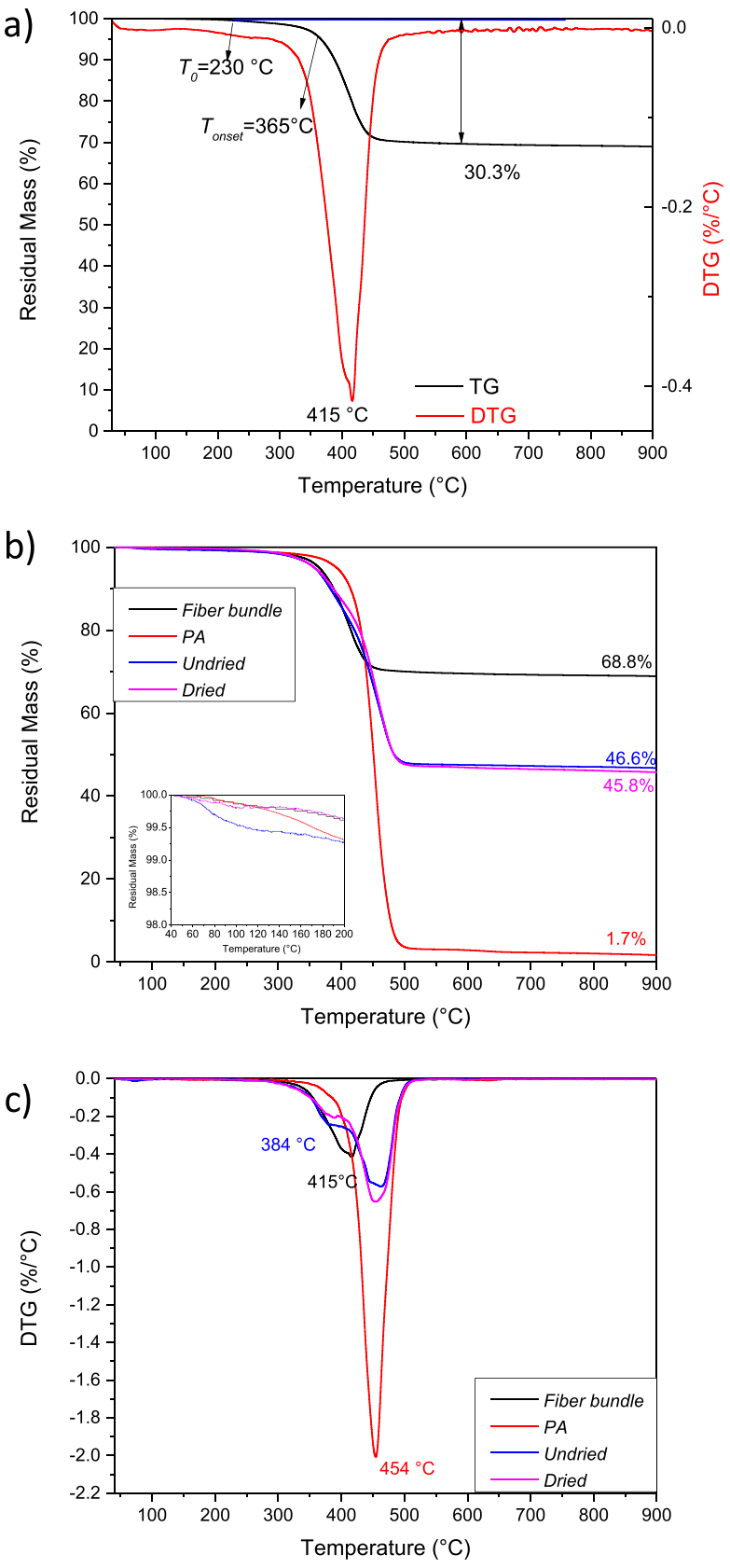

Fig. 3 Thermogravimetric curves of an impregnated fiber bundle (**a**), TG and DTG curves, residual mass (**b**). and derivative mass loss (**c**) curves of the fiber bundle, PA, and composites in the nitrogen atmosphere

Table 2 Mechanical properties of dried and undried tensile specimens

	σ_{tmax_avg} (MPa)	ε_{tmax_avg} (%)	E_{t_avg} (GPa)	Average weight loss (%)
Undried	340.49 ± 8.92[a]	0.82 ± 0.01[a]	41.13 ± 1.13[a]	-
Dried	392.78 ± 11.39[b]	0.93 ± 0.02[a]	43.33 ± 1.01[a]	0.51 ± 0.02

Different superscripts (a and b) within the same column indicate significant differences among formulations ($p < 0.05$)

Table 3 Mechanical properties of dried and undried flexural specimens

	σ_{fmax_avg} (MPa)	ε_{fmax_avg} (%)	E_{f_avg} (GPa)	Average weight loss (%)
Undried	133.74 ± 2.65[a]	0.56 ± 0.01[a]	31.77 ± 0.39[a]	-
Dried	151.06 ± 4.01[b]	0.59 ± 0.05 [a]	30.48 ± 0.83[a]	0.56 ± 0.07

Different superscripts (a and b) within the same column indicate significant differences among formulations ($p < 0.05$)

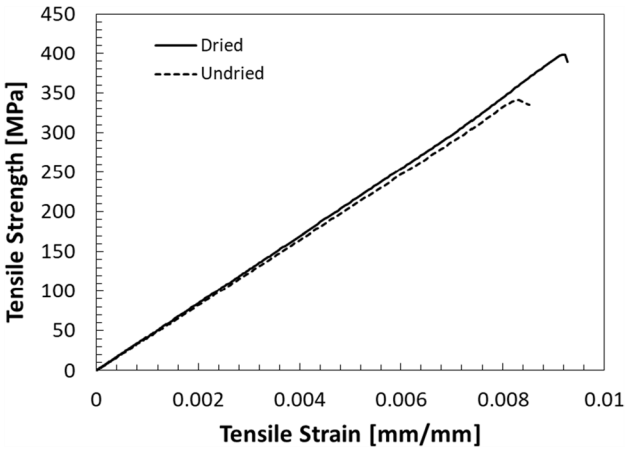

Fig. 4 Average tensile curves of dried and undried composite specimens

matrix to the fibers and, thus, to ensure the high mechanical properties of the examined composite material.

3.3 Flexural tests

A representative curve for both dried and undried specimens is displayed in Fig. 5, whereas the corresponding characteristic parameters are reported in Table 3.

The dried specimens exhibit an increase of the maximum flexural resistance (σ_{tmax_avg}) of 11.5% (significant differences ($p < 0.05$) after the post-drying process) while no particular variation was registered for flexural Young's

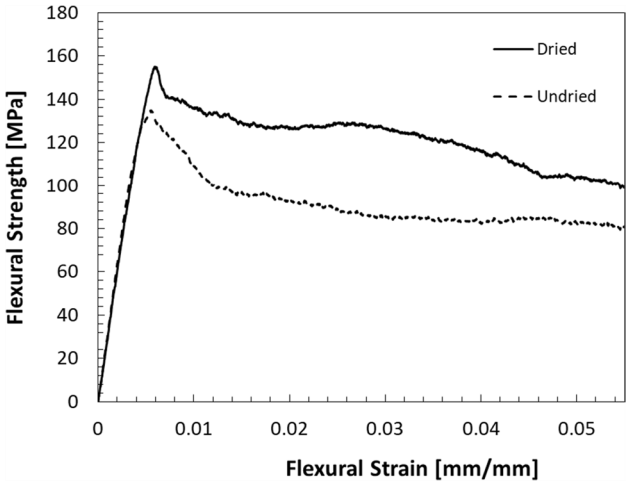

Fig. 5 Average flexural curves of dried and undried composite specimens

modulus (E_{t_avg}) and of the flexural strain at the peak stress point (ε_{tmax_avg}). The table also details the standard deviation for each parameter and the average weight loss relative to the drying process.

Similar results observed in tensile tests are also reflected in flexural tests, emphasizing the comprehensive enhancement of the material's mechanical properties. The drying process, by mitigating moisture-induced degradation, not only increases the material's resistance to tensile loads but also significantly enhances its ability to withstand flexural stresses. The latter increase further validates the crucial role of the drying process in preserving the structural integrity of the polymer and the fiber-matrix interface.

3.4 Optical and scanning electron microscope analyses

Figure 6 shows the optical micrography at 8× of a tested flexural specimen. A non-homogenous fracture surface can be seen, thus suggesting that multiple fracture mechanisms occurred, including matrix cracking, fiber-matrix debonding, and fiber breakage. This behavior can be caused by deposition defects and non-uniform impregnation of the fiber during the coextrusion process.

The presence of a non-homogenous fracture surface indicates the complexity of the failure process in the composite material. Such behavior can be attributed to several factors. The first one is matrix cracking**,** namely, the initial failure mechanism in composite materials under flexural loading. Matrix cracking can occur due to the brittle nature of the matrix material, which may not be able to withstand the tensile stresses induced during bending. These cracks can propagate, leading to further weakening of the composite structure. The second factor is fiber-matrix debonding**.** As

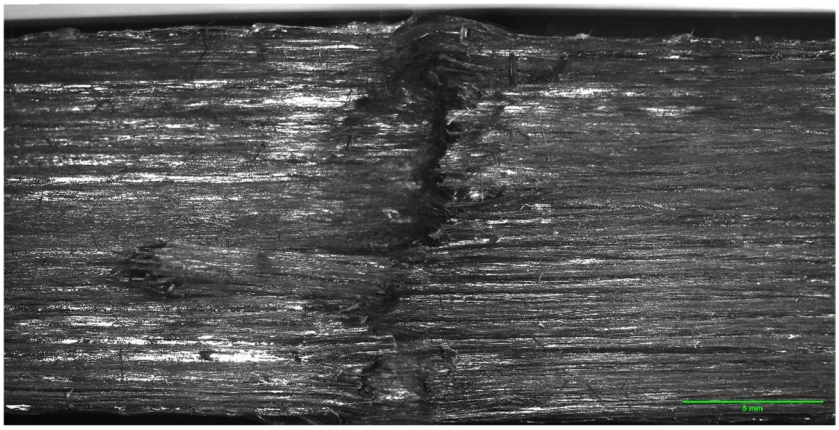

Fig. 6 Fractured surface 8× optical micrograph of flexural specimens

the matrix cracks, the load is transferred to the fibers. If the bonding between the fibers and the matrix is weak, debonding can occur. This debonding reduces the load transfer efficiency and contributes to the overall failure of the composite. The debonding observed in the micrograph suggests that there may have been issues with the fiber-matrix interface, possibly due to insufficient adhesion or improper curing processes. Lastly, the non-homogenous fracture surface is related to fiber breakage**.** Once the fibers are bearing the majority of the load, they may eventually reach their tensile strength limit and break. Fiber breakage is a critical failure mechanism as it signifies the ultimate load-bearing capacity of the composite. The observation of fiber breakage in the micrograph indicates that the fibers were subjected to high stress levels, which they could not withstand indefinitely.

The occurrence of these multiple fracture mechanisms can be linked to manufacturing imperfections. Specifically, deposition defects and non-uniform impregnation of the fibers during the coextrusion process are likely contributors. Deposition defects might include voids, uneven distribution of the resin, or contaminants that weaken the material structure. Non-uniform impregnation refers to the inconsistent distribution of the matrix material around the fibers, leading to areas with poor bonding and increased susceptibility to cracking and debonding.

Figure 7 shows the cross-section SEM images of a tensile specimen. In Fig. 7(a), the fiber bundle can be observed, along with the individual carbon fibers that constitute the fiber filament. The structure shows discontinuities between deposited bundles and the presence of macrovoids. Figure 7(b) is a higher magnification image and puts the evidence of the presence of microvoids between the single carbon fiber filaments.

The occurrence of both macrovoids and microvoids within the composite structure can be attributed to the 3D printing process. Specifically, macrovoids arise from defects during filament deposition, which results in unfilled spaces between adjacent extruded parts. These voids can form due to inconsistencies in the extrusion process, such as variations in temperature, pressure, or nozzle movement, leading to incomplete bonding between layers. On the other hand, microvoids, which are present within the filament bundles, indicate suboptimal impregnation during the extrusion phase. This suggests that the resin did not fully penetrate the

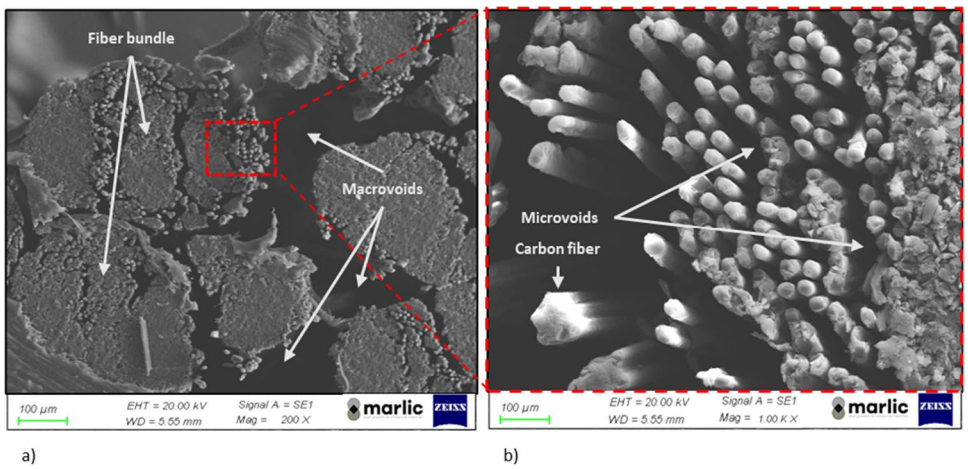

Fig. 7 **a**) 200× and **b**) 1000× SEM magnifications of 3D-printed composite

fiber bundles, possibly due to insufficient wetting or uneven distribution of the resin. These microvoids act as stress concentrators and significantly reduce the mechanical properties of the 3D-printed composite by creating weak points that can initiate cracks and propagate under load.

The presence of both macrovoids and microvoids can compromise the structural integrity and mechanical performance of the composite material, leading to reduced tensile strength and durability. Addressing these defects through process optimization, such as improving filament deposition techniques and ensuring better impregnation, is crucial for enhancing the quality and performance of 3D-printed composites. Future work should focus on refining the 3D printing parameters and incorporating real-time monitoring systems to detect and mitigate the formation of voids during the printing process.

4 Conclusion

In this study, the fabrication of a composite material for FDM 3D printing was investigated, with a particular emphasis on examining how moisture absorption affects its tensile and flexural properties. This 3D-printed composite material is engineered using continuous carbon fibers that are bonded with an epoxy resin and further impregnated with polyamide, thereby creating a dual-matrix composite structure. The TGA measurements permitted to determine the thermo-degradative profile and highlighted the different content of polymeric deposition on carbon fibers during the 3D printing process. The analysis revealed that the polyamide used in the 3D printing process, also if it is defined by the manufacturer with low hygroscopicity, is subjected to moisture absorption. However, using a drying process allows to remove up to 0.56% of this moisture by weight from the samples, leading to enhanced tensile and flexural properties, as evidenced by increased strength and stiffness. Furthermore, SEM analysis highlighted the presence of both microvoids and macrovoids in the 3D-printed composites, which not only led to a reduction of structural integrity but also potentially increased moisture absorption during the service phase. Moreover, it is critical to address the void content within the composites, as their presence can compromise the component's strength and amplify moisture absorption. For the latter, surface treatments such as spray and liquid coatings can be viable strategies to waterproof the surface and enhance the material's durability.

Future works will concentrate on optimizing 3D printing parameters to further refine the mechanical performance of these composites. More detailed studies will be conducted towards reducing void content and limiting moisture absorption in order to significantly elevate the quality and resilience of 3D-printed polyamide composites.

Acknowledgments The authors gratefully acknowledge the Marlic laboratory for the SEM analysis and Dr. Giuseppe Pandarese for his support in the experimental procedures.

Author contribution Andreozzi marina: writing, formal analysis, data curation, investigation. Serena Gentili: writing, formal analysis, data curation, investigation. Pietro Forcellese: supervision. Tiziano Bellezze: writing — reviewing and editing, supervision. Valeria Corinaldesi: supervision. Francesca Luzi: writing, formal analysis, data curation, investigation. Alessio Vita: methodology, investigation, writing—reviewing and editing, supervision.

Funding Open access funding provided by Università Politecnica delle Marche within the CRUI-CARE Agreement.

Declarations

Conflict of interest The authors declare no competing interests.

References

1. Iftekar SF, Aabid A, Amir A, Baig M (2023) Advancements and limitations in 3D printing materials and technologies: a critical review. Polymers 15:2519. https://doi.org/10.3390/POLYM15112519
2. Kristiawan RB, Imaduddin F, Ariawan D et al (2021) A review on the fused deposition modeling (FDM) 3D printing: filament processing, materials, and printing parameters. Open Eng 11:639–649. https://doi.org/10.1515/ENG-2021-0063/ASSET/GRAPHIC/J_ENG-2021-0063_FIG_003.JPG
3. Brenken B, Barocio E, Favaloro A et al (2018) Fused filament fabrication of fiber-reinforced polymers: a review. Addit Manuf 21:1–16. https://doi.org/10.1016/J.ADDMA.2018.01.002
4. Wickramasinghe S, Do T, Tran P (2020) FDM-based 3D printing of polymer and associated composite: a review on mechanical properties, defects and treatments. Polymers 12:1529. https://doi.org/10.3390/POLYM12071529
5. Zhao H, Liu X, Zhao W, Liu B (2019) An overview of research on FDM 3D printing process of continuous fiber reinforced composites. In Journal of Physics: Conference Series (1213, 5, 052037). IOP Publishing. https://doi.org/10.1088/1742-6596/1213/5/052037
6. Zhang H, Huang T, Jiang Q et al (2021) Recent progress of 3D printed continuous fiber reinforced polymer composites based on fused deposition modeling: a review. J Mater Sci 56:12999–13022. https://doi.org/10.1007/S10853-021-06111-W
7. Dul S, Fambri L, Pegoretti A (2021) High-performance polyamide/carbon fiber composites for fused filament fabrication: mechanical and functional performances. J Mater Eng Perform 30:5066–5085. https://doi.org/10.1007/S11665-021-05635-1/TABLES/11

8. Isobe T, Tanaka T, Nomura T, Yuasa R (2018) Comparison of strength of 3D printing objects using short fiber and continuous long fiber. IOP Conf Ser Mater Sci Eng 406:012042. https://doi.org/10.1088/1757-899X/406/1/012042
9. Yang C, Tian X, Liu T et al (2017) 3D printing for continuous fiber reinforced thermoplastic composites: mechanism and performance. Rapid Prototyp J 23:209–215. https://doi.org/10.1108/RPJ-08-2015-0098/FULL/XML
10. Prüß H, Vietor T (2015) Design for fiber-reinforced additive manufacturing. J Mech Des 137:111409. https://doi.org/10.1115/1.4030993/474831
11. Kabir SMF, Mathur K, Seyam AFM (2020) A critical review on 3D printed continuous fiber-reinforced composites: history, mechanism, materials and properties. Compos Struct 232:111476. https://doi.org/10.1016/J.COMPSTRUCT.2019.111476
12. Mashayekhi F, Bardon J, Berthé V et al (2021) Fused filament fabrication of polymers and continuous fiber-reinforced polymer composites: advances in structure optimization and health monitoring. Polymers 13:789. https://doi.org/10.3390/POLYM13050789
13. Cheng P, Peng Y, Li S et al (2023) 3D printed continuous fiber reinforced composite lightweight structures: a review and outlook. Compos B Eng 250:110450. https://doi.org/10.1016/J.COMPOSITESB.2022.110450
14. Piattaforma di produzione additiva industriale | Markforged. https://markforged.com/it/. Accessed 19 Jan 2024
15. Li N, Li Y, Liu S (2016) Rapid prototyping of continuous carbon fiber reinforced polylactic acid composites by 3D printing. J Mater Process Technol 238:218–225. https://doi.org/10.1016/j.jmatprotec.2016.07.025
16. Liu F, Ferraris E, Ivens J (2022) Mechanical investigation and microstructure performance of a two-matrix continuous carbon fibre composite fabricated by 3D printing. J Manuf Process 79:383–393. https://doi.org/10.1016/J.JMAPRO.2022.04.050
17. Adumitroaie A, Antonov F, Khaziev A et al (2019) Novel continuous fiber bi-matrix composite 3-D printing technology. Materials 12:3011. https://doi.org/10.3390/MA12183011
18. Azarov AV, Antonov FK, Vasil'ev VV et al (2017) Development of a two-matrix composite material fabricated by 3D printing. Polym Sci Ser D 10:87–90. https://doi.org/10.1134/S1995421217010026/METRICS
19. He Q, Wang H, Fu K, Ye L (2020) 3D printed continuous CF/PA6 composites: effect of microscopic voids on mechanical performance. Compos Sci Technol 191:108077. https://doi.org/10.1016/J.COMPSCITECH.2020.108077
20. Capela C, Ferreira JM, Costa JM et al (2016) Mechanical properties of injection-molded glass microsphere-reinforced polyamide. JMEP 25:4256–4265. https://doi.org/10.1007/S11665-016-2237-7
21. Di Pompeo V, Forcellese A, Mancia T et al (2021) Effect of geometric parameters and moisture content on the mechanical performances of 3D-printed isogrid structures in short carbon fiber-reinforced polyamide. J Mater Eng Perform 30:5100–5107. https://doi.org/10.1007/S11665-021-05659-7/FIGURES/8
22. Kodihalli Shivaprakash N, Ferraguto T, Panwar A et al (2019) Fabrication of flexible polymer molds for polymer microstructuring by roll-to-roll hot embossing. ACS Omega 4:12480–12488. https://doi.org/10.1021/ACSOMEGA.9B01468/ASSET/IMAGES/LARGE/AO-2019-014682_0008.JPEG
23. Hassan A, Rahman NA, Yahya R (2012) Moisture absorption effect on thermal, dynamic mechanical and mechanical properties of injection-molded short glass-fiber/polyamide 6,6 composites. Fibers Polym 13:899–906. https://doi.org/10.1007/S12221-012-0899-9
24. Dhakal HN, Zhang ZY, Richardson MOW (2007) Effect of water absorption on the mechanical properties of hemp fibre reinforced unsaturated polyester composites. Compos Sci Technol 67:1674–1683. https://doi.org/10.1016/J.COMPSCITECH.2006.06.019

Authors and Affiliations

Marina Andreozzi[1] · Serena Gentili[1] · Pietro Forcellese[2] · Tiziano Bellezze[2,3] · Valeria Corinaldesi[2,3] · Francesca Luzi[2,3] · Alessio Vita[1]

✉ Marina Andreozzi
m.andreozzi@pm.univpm.it

✉ Francesca Luzi
f.luzi@staff.univpm.it

[1] Department of Industrial Engineering and Mathematical Science, Polytechnic University of Marche, Via Brecce Bianche, 12 Ancona, Italy

[2] Department of Science and Engineering of Matter, Environment and Urban Planning (SIMAU), Polytechnic University of Marche, Via Brecce Bianche, 12 Ancona, Italy

[3] National Interuniversity Consortium of Materials Science and Technology (INSTM), Florence, Italy